

Quantum phase transitions in systems of parallel quantum dots

Rok Žitko¹ and Janez Bonča²

¹*J. Stefan Institute, Ljubljana, Slovenia*

²*Faculty of Mathematics and Physics, University of Ljubljana, Ljubljana, Slovenia*

(Received 15 November 2007; published 18 December 2007)

We study the low-temperature transport properties of systems of parallel quantum dots described by the N -impurity Anderson model. We calculate the quasiparticle scattering phase shifts, spectral functions, and correlations as a function of the gate voltage for N up to 5. For any N , the conductance at the particle-hole symmetric point is unitary. For $N \geq 2$, a transition from ferromagnetic to antiferromagnetic impurity spin correlations occurs at some gate voltage. For $N \geq 3$, there is an additional transition due to an abrupt change in average impurity occupancy. For odd N , the conductance is discontinuous through both quantum phase transitions, while for even N only the magnetic transition affects the conductance. Similar effects should be experimentally observable in systems of quantum dots with ferromagnetic conduction-band-mediated interdot exchange interactions.

DOI: 10.1103/PhysRevB.76.241305

PACS number(s): 73.63.Kv, 72.10.Fk, 72.15.Qm

Parallel double quantum dots in semiconductor heterostructures exhibit many interesting quantum effects at low temperatures, such as the formation of molecular states, Aharonov-Bohm oscillations, phase lapses, and the Kondo effect.¹⁻⁷ They are also predicted to exhibit quantum phase transitions of different kinds.^{8,9} Interdot exchange interactions, both ferromagnetic (FM) and antiferromagnetic (AFM), play a central role in such systems.¹⁰⁻¹⁷ Furthermore, the phase-coherent electron transport leads to various possible interference effects and Fano antiresonances.¹⁸⁻²¹ Recently, few-electron triple-quantum-dot structures have been fabricated^{22,23} and even more complex multidot nanostructures can also be assembled in principle. It is thus appropriate to endeavor to study phenomena which occur in multiple-dot systems.

The simplest N -impurity Anderson model for several dots embedded in parallel between two conduction leads in a left-right symmetric way [see the insets in Fig. 1(a)] is defined by $H = H_b + \sum_{i=1}^N H_i$, where H_b describes a band with a constant density of states $\rho = 1/2D$ ($2D$ is the bandwidth) and

$$H_i = \delta n_i + \frac{U}{2}(n_i - 1)^2 + V \sum_{k\sigma} (c_{k\sigma}^\dagger d_{i\sigma} + \text{H.c.}). \quad (1)$$

The parameter $\delta = \epsilon + U/2$ is related to the gate voltage, U is the electron-electron repulsion, and we assume that all impurities hybridize with the same left-right symmetric combinations of states from both leads with a constant hybridization function $\Gamma = \pi\rho V^2$; this corresponds to taking the limit of small interdot separation.⁸ The interdot tunneling coupling and capacitive coupling (interdot charge repulsion) are assumed small and all dots are equivalent: the system thus has S_N -symmetric group symmetry of all possible permutations of dot labels i . At the particle-hole (p-h) symmetric point, $\delta = 0$, and for $U/\pi\Gamma \gg 1$, the conduction-band-mediated interdot exchange interaction induces FM alignment of the impurity spins, and the system undergoes the spin- $N/2$ Kondo effect ending up in an underscreened strong-coupling (SC) Fermi liquid fixed point with residual spin $N/2 - 1/2$.^{8,11,12,15,24-27} For very large δ/U , the impurities are

unoccupied and the system is in the frozen-impurity (FI) fixed point with no residual spin. In the single-impurity ($N=1$) case, the SC and FI fixed points lie on the same line of fixed points and they differ only in the strength of the potential scattering.²⁸ For $N \geq 2$, however, the SC and FI lines of fixed points are qualitatively different (each corresponding to a different residual spin) and must be separated by at least one quantum phase transition (QPT).²⁹

A reliable technique to study the low-temperature properties of coupled quantum dot systems is the numerical renormalization group (NRG).^{30,31} In this Rapid Communication, we show that, for any $N \geq 2$, the FM alignment collapses at some critical value δ_{c1} and that for $\delta > \delta_{c1}$ the interimpurity spin-spin correlations are AFM. For $N \geq 3$, there is precisely one additional QPT at slightly higher δ_{c2} related to an abrupt change in the average impurity occupancy. Certain of these phase transitions can be easily detected in zero-bias conductance measurements.

Conductance. The on-site energy ϵ can be regulated using the gate voltages to tune the charge state (occupancy) on the dots. Gate-voltage-dependent conductance is shown in Fig. 1(a) for $N=1, \dots, 5$ for a range of magnetic field strengths. The conductance is calculated as $G = G_0/2 \sum_{\sigma=\uparrow, \downarrow} \sin^2 \delta_{\text{qp}}^\sigma$ where $G_0 = 2e^2/h$ is the conductance quantum³² and the quasiparticle scattering phase shifts $\delta_{\text{qp}}^\sigma$ are extracted from the NRG excitation spectra.

At $\delta=0$, the systems are fully conducting at zero field and there is a wide plateau of high conductance associated with the spin- $N/2$ Kondo effect.⁸ While the $N=1$ system smoothly crosses over from the Kondo regime to the nonconducting FI regime, in the multi-impurity case we observe sharp discontinuities: one discontinuity for N even and two discontinuities for N odd. The conductance culminates in a unitary peak slightly below $\epsilon=0$ (i.e., below $\delta/U=1/2$) for all $N \geq 2$. The origin of this peak is simply potential scattering. The magnetic field B has a strong effect on the Kondo plateau: the conductance is significantly reduced as soon as B is of the order of the Kondo temperature T_K . The potential scattering peak is affected only by extremely high fields of the order of U .

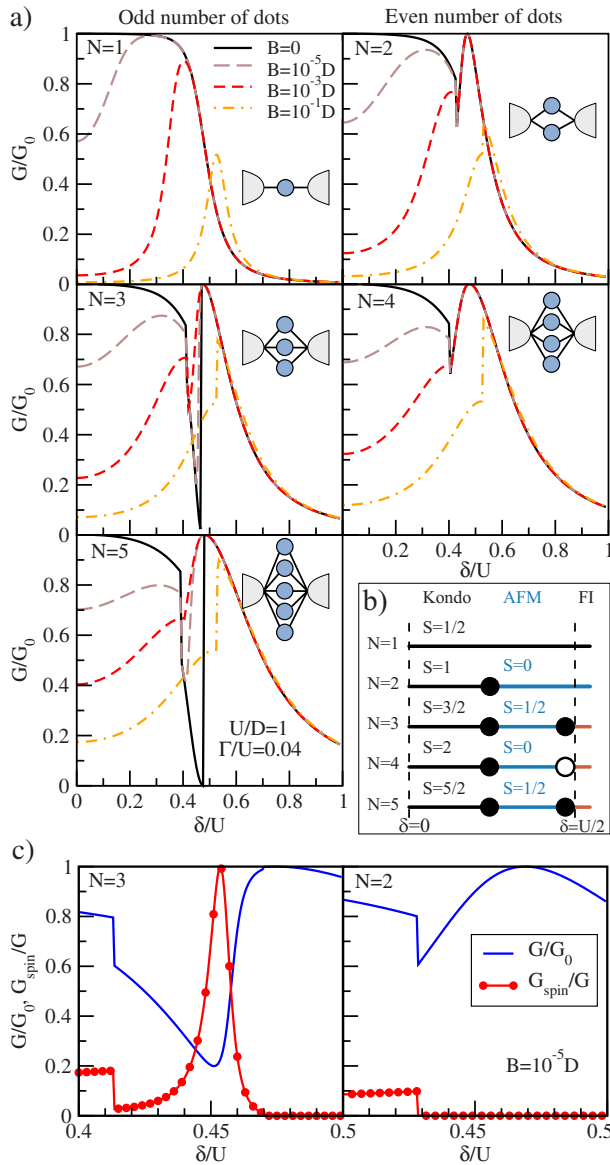


FIG. 1. (Color online) (a) Zero-temperature conductance through systems of N parallel quantum dots as a function of the gate voltage for a range of magnetic fields. The in-plane field leads only to Zeeman splitting; no magnetic flux pierces the rings formed by pairs of dots. $\Lambda=4$; NRG iterations were performed until the zero-temperature limit was reached. $T_K=3.3 \times 10^{-6}D$ (for $N=2$). The magnetic field is measured in units of $g\mu_B$. Only $\delta>0$ is shown due to the symmetry of the problem. (b) Zero-temperature phase diagram delimiting the different regimes as a function of the gate voltage. Filled circles (●) correspond to phase transitions visible in conductance, while the empty circle (○) denotes the phase transition with no associated conductance discontinuity. (c) Conductance and spin conductance in small magnetic field in the transition region.

Quantum phase transitions. Conductance discontinuities find their counterparts in the jumps of the total impurity occupancy and spin-spin correlation $\langle S_i \cdot S_j \rangle$ [Fig. 2(a)]; a new feature, however, is the existence of two points of discontinuity for $N=4$ while the conductance exhibits only one. In the Kondo regime for $\delta < \delta_{c1}$, the systems are nearly half

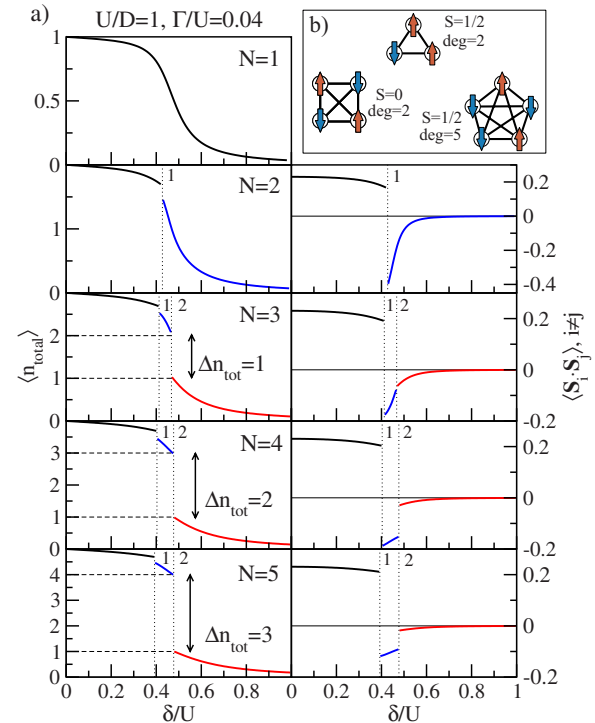


FIG. 2. (Color online) (a) Total occupancy (charge) and spin-spin correlation between pairs of spins as a function of the gate voltage. (b) Schematic representations of the spin configurations in the intermediate AFM ordered phases, their total spins, and degeneracies for $N \geq 3$.

filled and spins are aligned.⁸ As we cross δ_{c1} , the occupancy abruptly decreases and the spin correlations turn from FM to AFM. For $N \geq 3$, a second discontinuity occurs at somewhat higher δ_{c2} ; its characteristic property is the occupancy jump by almost exactly $N-2$, from $N-1$ to 1. According to the Friedel sum rule, a change in the occupancy by n is mirrored in a change of the scattering phase shift by $\Delta\delta_{\text{qp}}=n\pi/2$. This explains the conductance jump from $G=0$ to $G=G_0$ in the case of odd $N \geq 3$ and the absence of the second conductance discontinuity for even $N \geq 4$. It is remarkable that the second QPT occurs precisely at the point where the conductance is extremal.

The discontinuities originate from an interplay of the Ruderman-Kittel-Kasuya-Yosida RKKY interactions,⁸ the presence of the bound states in the continuum,^{11,19,21} and the occupancy switching.³³⁻³⁵ We note that only the symmetric state described by the operator $d_{\text{sym}}^\dagger = 1/\sqrt{N} \sum_i d_i^\dagger$ hybridizes directly with the conduction band, while all asymmetric states are decoupled. A close-up of the points of discontinuity for $N=2,3$ is shown in Fig. 3. As we move away from $\delta=0$, only the symmetric state is depopulated until we reach δ_{c1} . At this point, the asymmetric levels are depopulated and the symmetric level repopulated (up to exactly 1 for $N=2$); such occupancy switching stems from the competition between the Γ -dependent coupling of dots to the conduction band and the charging energy U .³⁵ Between δ_{c1} and δ_{c2} , the occupancy of all states decreases until at δ_{c2} another charge oscillation occurs in which the occupancy of the asymmetric states plummets. Both transitions can be classified as first-

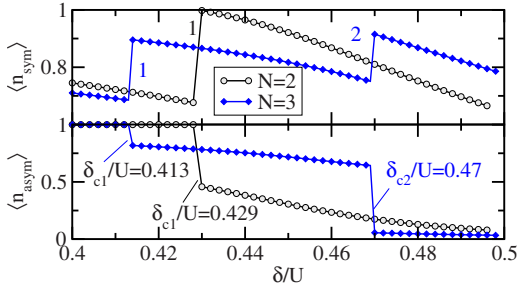


FIG. 3. (Color online) Expectation values in the symmetric and asymmetric bases for $N=2$ and 3 systems. The asymmetric combination of states considered is $d_{\text{asym}}^{\dagger}=1/\sqrt{2}(d_1^{\dagger}-d_2^{\dagger})$.

order boundary quantum phase transitions (level crossings);³³ the schematic phase diagram shown in Fig. 1(b).

For $\delta_{c1} \leq \delta$ ($N=2$) and for $\delta_{c1} < \delta < \delta_{c2}$ ($N \geq 3$), each spin interacts with every other spin antiferromagnetically with an equal strength. The ground state of such an effective Heisenberg Hamiltonian consists of one singlet for $N=2$, two degenerate doublets for $N=3$, two degenerate singlets for $N=4$, etc.³⁶ [see Fig. 2(b)]. Results for magnetic susceptibility and entropy demonstrate that in odd- N systems the spin degree of freedom is screened by the spin-1/2 Kondo effect and that the residual entropy is the logarithm of the additional degeneracy of the ground-state spin multiplets. This implies that in this phase (for $N \geq 3$) there are several equally probable ways for the electron spin ordering. Consequently, this “magnetic-frustration” phase is sensitive to the breaking of the S_N symmetry between the impurities, which lifts the degeneracy. For odd N and for weak magnetic field, the transmitted current in this regime becomes fully spin polarized at some gate voltage (it should be noted that in the presence of magnetic field the phase transition at δ_{c2} is replaced by a crossover²⁷); see the plot of G_{spin}/G where $G_{\text{spin}}=G_0/2(\sin^2 \delta_{\text{qp}}^{\uparrow}-\sin^2 \delta_{\text{qp}}^{\downarrow})$ is the spin current and G is the total (charge) current, Fig. 1(c). Thus the $N=3$ device might function as a spin filter.^{27,37,38}

For decreasing interaction strength U , the discontinuous features in the conduction plots narrow down and disappear for $U=0$; at this point the conductance curve consists of a single Lorentzian peak of width $N\Gamma$ centered at $\delta=0$. This demonstrates that the conductance discontinuities are adiabatically connected with the ghost Fano resonances (bound states in the continuum) found in the systems of noninteracting parallel dots.^{19,21}

Robustness. Finite interdot charge repulsion U_{12} and interdot hopping t have little effect as long as $U_{12} \ll U$, $t \ll U - U_{12}$, and $4t^2/(U - U_{12}) \ll J_{\text{eff}}$, where J_{eff} is the effective conduction-band-mediated interimpurity exchange interaction.⁸ The first two constraints are easily met in experiments³⁹ and together they imply the third unless J_{eff} is very small.

The S_N symmetry is broken if the strengths of the hybridization Γ_i of each impurity to the conduction band are made unequal, or if different gate voltages ϵ_i are applied to the dots. This leads to smearing of the discontinuities in the

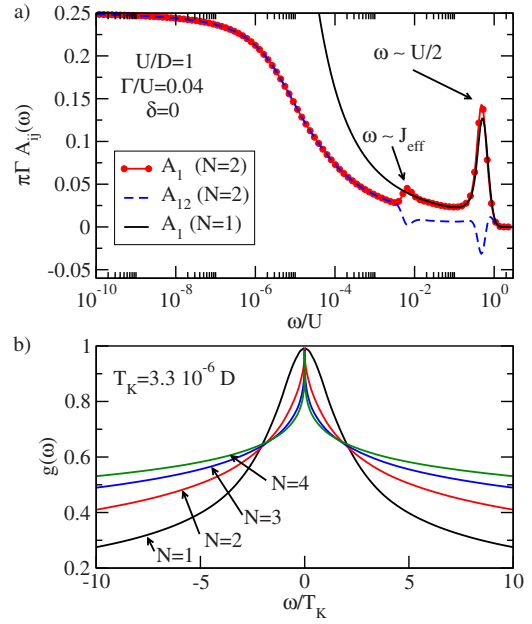


FIG. 4. (Color online) (a) Normalized spectral function $\pi\Gamma A_{ij}(\omega)$ and (b) function $g(\omega)=\pi\Gamma \sum_{ij} A_{ij}(\omega)$.

occupancy and correlation functions; nevertheless, the discontinuities in the conductance curves persist (i.e., level crossings still occur). Curiously, the first discontinuity in the conductance no longer coincides with the sign change of $\langle \mathbf{S}_i \cdot \mathbf{S}_j \rangle$.

For a generic problem of parallel dots, in particular if left-right (LR) and S_N symmetries are weakly broken, the antisymmetric combinations of the conduction band electrons become relevant and we need to consider the full N -impurity two-channel model. In this case, the spin- $N/2$ Kondo effect is followed by another stage of the Kondo screening to $S=N/2-1$ at significantly lower Kondo temperature $T_K^{(2)}$. This leads to a phase shift of $\pi/2$ in the odd scattering channel and the zero-temperature conductance in the “Kondo regime” becomes very small³² (see Refs. 15, 20, and 27 for the $N=2$ case). Nevertheless, if LR symmetry breaking is weak, the conductance curves shown in Fig. 1 are a good approximation for the finite-temperature conductance in the experimentally relevant $T_K \gg T \gg T_K^{(2)}$ range.

Spectral functions. In Fig. 4(a), we plot spectral functions $A_{ij}(\omega)=-1/(2\pi)\text{Im}(G_{ij}^r+G_{ji}^r)$ for $N=1$ and 2 at the p-h symmetric point.⁴⁰ The diagonal spectral functions $A_i=A_{ii}$ represent the on-site density of states, while the out-of-diagonal spectral functions A_{ij} with $i \neq j$ are related to the processes where one electron is injected at one site and later extracted at a different site. The peak in A_i at $U/2$ is the familiar charge excitation peak that is observed for all N ; for $N \geq 2$ a small negative peak appears in the out-of-diagonal spectral densities A_{ij} . Additional features for $J_{\text{eff}} \lesssim \omega \lesssim U$ are related to the magnetic alignment:^{16,41} the diagonal spectral function exhibits a broad hump which peaks at $\sim J_{\text{eff}}$, while the out-of-diagonal spectral function exhibit a slight depression. For $\omega < J_{\text{eff}}$, when the spins align, all A_{ij} curves merge into a Kondo resonance.

In Fig. 4(b), we plot the symmetrized and normalized

spectral density function $g(\omega) = \pi \Gamma \sum_{ij} A_{ij}$, which determines the conductance through the dots as $G = G_0 \int (-\partial f / \partial \omega) g d\omega$, where f is the Fermi-Dirac distribution function.^{40,42} In a simple approximation, $g(\omega)$ at $\omega = T$ indicates the conductance through the system at temperature T . Only for $N=1$ is the approach to the unitary conductance at $T=0$ rapid (quadratic), as expected for regular Fermi liquid systems. For $N \geq 2$, the Kondo resonance is cusplike and the approach to the unitary conductance is very slow (logarithmic).^{24,43} This is characteristic for underscreened Kondo systems, which behave as singular Fermi liquids.^{43,44}

Conclusion. For $N \geq 3$, the N -impurity Anderson model undergoes two phase transitions. The first transition separates the spin alignment and the associated spin- $N/2$ Kondo

screening from the spin antialignment with magnetic frustration and (for odd N) Kondo screening of the spin-1/2 moment. The second transition reflects the instability of the phases with the occupancy in the interval $1 < \langle n_{\text{tot}} \rangle < N-1$. Furthermore, for odd N the system abruptly switches from being fully conducting to zero conductance; this would facilitate the experimental observation of similar effects in quantum dot systems and might even have applications as a switch or a transistor with very high on-off ratio. In addition, the odd N system appears as a possible realization of a gate-voltage-switchable spin filter device.

The authors acknowledge the financial support of the SRA under Grant No. P1-0044.

- ¹A. W. Holleitner, A. Chudnovskiy, D. Pfannkuche, K. Eberl, and R. H. Blick, *Phys. Rev. B* **70**, 075204 (2004).
- ²T. Hatano, M. Stopa, and S. Tarucha, *Science* **309**, 268 (2005).
- ³M. Sigrist, A. Fuhrer, T. Ihn, K. Ensslin, S. E. Ulloa, W. Wegscheider, and M. Bichler, *Phys. Rev. Lett.* **93**, 066802 (2004).
- ⁴M. Sigrist, T. Ihn, K. Ensslin, D. Loss, M. Reinwald, and W. Wegscheider, *Phys. Rev. Lett.* **96**, 036804 (2006).
- ⁵J. C. Chen, A. M. Chang, and M. R. Melloch, *Phys. Rev. Lett.* **92**, 176801 (2004).
- ⁶N. J. Craig, J. M. Taylor, E. A. Lester, C. M. Marcus, M. P. Hanson, and A. C. Gossard, *Science* **304**, 565 (2004).
- ⁷S. Sasaki, S. Kang, K. Kitagawa, M. Yamaguchi, S. Miyashita, T. Maruyama, H. Tamura, T. Akazaki, Y. Hirayama, and H. Takayanagi, *Phys. Rev. B* **73**, 161303(R) (2006).
- ⁸R. Žitko and J. Bonča, *Phys. Rev. B* **74**, 045312 (2006).
- ⁹L. G. G. V. Dias da Silva, N. P. Sandler, K. Ingersent, and S. E. Ulloa, *Phys. Rev. Lett.* **97**, 096603 (2006).
- ¹⁰R. López, R. Aguado, and G. Platero, *Phys. Rev. Lett.* **89**, 136802 (2002).
- ¹¹R. López, D. Sánchez, M. Lee, M.-S. Choi, P. Simon, and K. Le Hur, *Phys. Rev. B* **71**, 115312 (2005).
- ¹²Y. Utsumi, J. Martinek, P. Bruno, and H. Imamura, *Phys. Rev. B* **69**, 155320 (2004).
- ¹³P. Simon, R. López, and Y. Oreg, *Phys. Rev. Lett.* **94**, 086602 (2005).
- ¹⁴P. Simon, *Phys. Rev. B* **71**, 155319 (2005).
- ¹⁵H. Tamura and L. Glazman, *Phys. Rev. B* **72**, 121308(R) (2005).
- ¹⁶M. G. Vavilov and L. I. Glazman, *Phys. Rev. Lett.* **94**, 086805 (2005).
- ¹⁷G. Chiappe and A. A. Aligia, *Phys. Rev. B* **70**, 129903(E) (2004).
- ¹⁸H. Lu, R. Lü, and B. F. Zhu, *Phys. Rev. B* **71**, 235320 (2005).
- ¹⁹M. L. Ladrón de Guevara and P. A. Orellana, *Phys. Rev. B* **73**, 205303 (2006).
- ²⁰C. Karrasch, T. Enns, and V. Meden, *Phys. Rev. B* **73**, 235337 (2006).
- ²¹M. L. Ladrón de Guevara, F. Claro, and P. A. Orellana, *Phys. Rev. B* **67**, 195335 (2003).
- ²²M. Korkusinski, I. P. Gimenez, P. Hawrylak, L. Gaudreau, S. A. Studenikin, and A. S. Sachrajda, *Phys. Rev. B* **75**, 115301 (2007).
- ²³L. Gaudreau, S. A. Studenikin, A. S. Sachrajda, P. Zawadzki, A. Kam, J. Lapointe, M. Korkusinski, and P. Hawrylak, *Phys. Rev. Lett.* **97**, 036807 (2006).
- ²⁴A. Posazhennikova and P. Coleman, *Phys. Rev. Lett.* **94**, 036802 (2005).
- ²⁵C. Jayaprakash, H. R. Krishna-murthy, and J. W. Wilkins, *Phys. Rev. Lett.* **47**, 737 (1981).
- ²⁶W. Hofstetter and H. Schoeller, *Phys. Rev. Lett.* **88**, 016803 (2001).
- ²⁷M. Pustilnik and L. Borda, *Phys. Rev. B* **73**, 201301(R) (2006).
- ²⁸H. R. Krishna-murthy, J. W. Wilkins, and K. G. Wilson, *Phys. Rev. B* **21**, 1044 (1980).
- ²⁹M. Vojta, *Philos. Mag.* **86**, 1807 (2006).
- ³⁰K. G. Wilson, *Rev. Mod. Phys.* **47**, 773 (1975).
- ³¹R. Bulla, T. Costi, and T. Pruschke, arXiv:cond-mat/0701105.
- ³²M. Pustilnik and L. I. Glazman, *Phys. Rev. Lett.* **87**, 216601 (2001).
- ³³V. M. Apel, M. A. Davidovich, G. Chiappe, and E. V. Anda, *Phys. Rev. B* **72**, 125302 (2005).
- ³⁴M. Sindel, A. Silva, Y. Oreg, and J. von Delft, *Phys. Rev. B* **72**, 125316 (2005).
- ³⁵P. G. Silvestrov and Y. Imry, *Phys. Rev. Lett.* **85**, 2565 (2000).
- ³⁶A. J. van der Sijs, *Phys. Rev. B* **48**, 7125 (1993).
- ³⁷M. E. Torio, K. Hallberg, S. Flach, A. E. Miroshnichenko, and M. Titov, *Eur. Phys. J. B* **37**, 399 (2004).
- ³⁸A. A. Aligia and L. A. Salguero, *Phys. Rev. B* **70**, 075307 (2004).
- ³⁹T. Hatano, M. Stopa, T. Yamaguchi, T. Ota, K. Yamada, and S. Tarucha, *Phys. Rev. Lett.* **93**, 066806 (2004).
- ⁴⁰R. Žitko and J. Bonča, *Phys. Rev. B* **74**, 224411 (2006).
- ⁴¹R. Žitko and J. Bonča, *Phys. Rev. Lett.* **98**, 047203 (2007).
- ⁴²Y. Meir and N. S. Wingreen, *Phys. Rev. Lett.* **68**, 2512 (1992).
- ⁴³W. Koller, A. C. Hewson, and D. Meyer, *Phys. Rev. B* **72**, 045117 (2005).
- ⁴⁴P. Mehta, N. Andrei, P. Coleman, L. Borda, and G. Zarand, *Phys. Rev. B* **72**, 014430 (2005).